Moisture induced weathering of volcanic tuffstone

Lubelli, Barbara; Nijland, Timo G.; Tolboom, Hendrik Jan

DOI
10.1016/j.conbuildmat.2018.08.002

Publication date
2018

Document Version
Final published version

Published in
Construction and Building Materials

Construction and Building Materials 187 (2018) 1134–1146

Contents lists available at ScienceDirect

Construction and Building Materials

journal homepage: www.elsevier.com/locate/conbuildmat

Moisture induced weathering of volcanic tuffstone

Barbara Lubelli [a,*], Timo G. Nijland [b], Hendrik-Jan Tolboom [c]

[a] Faculty of Architecture, Delft University of Technology, Delft, The Netherlands
[b] TNO, Delft, The Netherlands
[c] Cultural Heritage Agency, Amersfoort, The Netherlands

HIGHLIGHTS

- The response of Weibern and Ettringen tuff stones to moisture has been investigated.
- A purpose-made weathering test was carried out to simulate the wetting-drying process.
- Pore size, porosity, moisture transport and hygric behaviour of both stones were measured.
- Both tuff stones have an extreme dilation in response to RH changes and to wetting.
- All results show that moisture gradients in tuff elements may enhance decay in this stone.

GRAPHICAL ABSTRACT

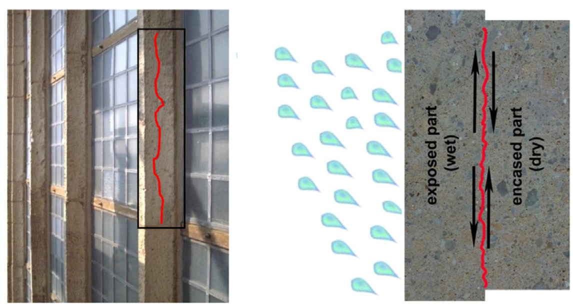

ARTICLE INFO

Article history:
Received 29 January 2018
Received in revised form 12 July 2018
Accepted 1 August 2018
Available online 19 August 2018

Keywords:
Tuffstone
Ettringen tuff
Weibern tuff
Weathering
Hygric dilation
Porosity
Pore size
Environmental X-ray diffraction

ABSTRACT

Tuffstone elements with a large length/width ratio often suffer damage in the form of cracks parallel to the surface and spalling of the outer layer. This study aimed at verifying if this damage may be the result of a differential dilation between parts with different moisture content. The research, carried out on Ettringen and Weibern tuff, comprised a weathering test and measurements of porosity, moisture transport and hygric behaviour of the stones, supplemented by environmental X-ray diffraction analyses. Results support the hypothesis that moisture gradients in tuff elements may enhance decay in this stone.

1. Introduction

Zeolitized volcanic tuffstones have been used in many regions and countries all over the world, including Japan, Turkey, Middle America, Italy, Hungary and northwestern Europe [1,2]. Volcanic tuffstones from the Eifel region (Germany), including Römer, Weibern and Ettringen tuffstone, have widely been used in the Netherlands [3,4], northwestern Germany [5,6], western Denmark [7] and, rarely, Belgium [8]. Römer tuff has been used since Roman times in Germany, the Netherlands and Belgium. Use was resumed in the period of Romanesque architecture, in which it was also used in Denmark. With a few earlier exceptions, Weibern tuff was used in the 15th century and from the 19th century till half

* Corresponding author.
E-mail address: b.lubelli@tudelft.nl (B. Lubelli).

https://doi.org/10.1016/j.conbuildmat.2018.08.002
0950-0618/

20th century, the latter corresponding to the period of use of Ettringen tuff. Both Ettringen and Weibern tuff are still in use for restoration purposes. Tuffstone is often regarded, not always correctly, as a stone with a limited durability; this statement, however, is contradicted by presence of building time Römer tuff on several Romanesque churches in the Netherlands. The limited durability often attributed to tuff stone may also derive from the fact that the different damage mechanisms affecting tuffstone have not been fully elucidated yet.

Besides damage types such as powdering of the surface layer and scaling of the outer surface, typical for weathering due freeze-thaw and salt crystallization, tuffstone elements with a relatively high length to width ratio, as e.g. mullions and (window) sills, often develop single longitudinal crack in the protruding, exposed part of the element, finally resulting in spalling of the outer layer (Figs. 1 and 2). Less commonly, disintegration into fragments of several centimetre to decimetre size may occur. This type of damage is mostly observed on Ettringen tuff elements (Fig. 1) and only rarely in Weibern tuff (Fig. 2). It is unclear whether this is due to the nature of the stone itself, or, at least in part, an artefact of the architectural use (Römer tuff is, for example, never used as larger elements in mullions or sills, but nearly always in blocks).

The weathering of zeolitized volcanic tuffstones, including the effects of frost and salt decay, have widely been researched in the past, e.g. on stone varieties from the Eifel, Germany [5,8–13], Campania/Naples, Italy [14–17] and elsewhere [e.g. 18,19]. These

Fig. 1. Typical longitudinal cracking (left) and final damage (right) in mullions of Ettringen tuff at the tower of Eusebius' church in Arnhem, The Netherlands.

Fig. 2. Typical longitudinal cracking (left) and final damage (right) in mullions of Weibern tuff at the nave of St. Peter's church in Leiden, The Netherlands.

damage mechanisms, however, do not explain the above described decay patterns. One of the hypotheses is that cracks are due to the hygric-mechanic behaviour of the tuffstone. Despite some studies exist on the hygric behaviour of Weibern tuff [12] and the relationship between hygric expansion and micropores [13], the cause of the above described decay patterns is still unclear.

Rhenish tuffstone typically has a high porosity and a bimodal pore size distribution, with both very coarse and very fine pores; these properties result in a high and fast water absorption and a slow drying. When the protruding part gets wet due to rain and dry afterwards, differences in moisture content and consequent hygric dilation may develop between the exposed and the encased part of the stone, possibly leading to stresses at the interface. These stresses may cause damage in the form of longitudinal cracks at the interface and spalling of the outer layer of the stone. This hypothesis has been investigated in this research for both Ettringen and Weibern tuffstone. A purpose-made weathering test was carried out to simulate the wetting-drying process due to rain and sun [20].

An alternative hypothesis that has been put forward, is that initiation of cracks already occurs during tooling by a stone mason, and progressively develops in time. To evaluate this hypothesis, part of the samples, both mullions and sills, have been chiselled.

Additionally, stone properties relevant to this damage mechanism, (e.g. water absorption and drying, porosity and pore size distribution, and hygric behaviour of the stones), have been investigated.

2. Materials and methods

Fresh quarry Ettringen and Weibern tuff was obtained from a stone mason's company. Both tuff stones are zeolitized deposits from the Riedener caldera in the Eifel area, Germany [21,22].

The test plan consisted of a weathering test, aiming at simulating in laboratory the wet-dry cycles occurring in the field, and a series of characterization tests, some of them carried out before and after the weathering test. Specimens of different sizes were used for the tests: cubes, prisms, small scale mullions and window sills; part of these were simply cut by a saw and left untooled. (Fig. 3); another part of the specimens were made in a traditional way by hand by a stone mason and tooled by a chisel (Fig. 4) for

Fig. 3. Examples of cut mullion and window sill.

Fig. 4. Making of a mullion by hand (left) and example of a tooled mullion (right).

Table 1
Characterization methods (B = before weathering test; A = after weathering test) and type, size and number of specimens tested.

Test method	Type of specimen	Size	B/A	Replica's per stone type
Water absorption	Cubes	$10 \times 10 \times 10\ cm^3$	B	3
Drying at 20 °C/50% RH	Cubes	$10 \times 10 \times 10\ cm^3$	B	3
Porosity under vacuum	Cubes	$4 \times 4 \times 4\ cm^3$	B	3
MIP	Little pieces	$\cong 1\ cm^3$	B	2
N_2 adsorption	Little pieces	$\cong 1\ cm^3$	B	2
Flexural & compressive strength	Prisms	$4 \times 4 \times 16\ cm^3$	B, A	5B + 5A
Macroscopic observations on samples impregnated with fluorescent resin	Cubes (toold and untooled)	$10 \times 10 \times 10\ cm^3$	B, A	B:2; A:2
	Mullions (tooled and untooled)	See Fig. 3	A	2
	Window sills (tooled and untooled)	See Fig. 3	A	2
Polarized and Fluorescent microscopy (PFM)	Part of cubes	$\cong 3 \times 5$ cm	B	1
	Part of mullions	$\cong 3 \times 5$ cm	B, A	B:1; A:1
	Part of tooled mullions	$\cong 3 \times 5$ cm	B, A	B:1; A:1
	Part of window sills	$\cong 3 \times 5$ cm	A	1
	Part of tooled window sills	$\cong 3 \times 5$ cm	A	1
Hygric dilation and adsorption	Prisms	$16 \times 4 \times 4\ cm^3$	B	3
Hygric dilation (RH cycles)	Prisms	$16 \times 4 \times 4\ cm^3$	B	1
Thermal dilation (20–40 °C)	Prisms	$16 \times 4 \times 4\ cm^3$	B	3
X-ray diffraction	Powder	n.a.	B	2
X-ray diffraction (RH cycles)	Powder	n.a.	B	1

the reasons given above. Type, number and size of specimens and test methods used in this research are summarized in Table 1.

The mineralogical and petrographical properties of the tuff stones were investigated by polarized and fluorescent light microscopy (PFM). Specimens were prepared by impregnating the stone under vacuum with a UV-fluorescent resin and then cutting and polishing the samples to obtain thin sections of 25–30 μm thickness. PFM observations were also carried out, together with fluorescent macroscopic observations (FMA, i.e. analysis of polished slabs impregnated with an UV-fluorescent resin), to assess the appearance of damage (cracks, mineralogical changes, etc.) after the weathering test.

The mineralogical composition of the tuffstone was further investigated by X-ray diffraction analysis (XRD) on ground tuffstone samples. Because the type of zeolites present is thought to possibly play a role in the damage process, samples were prepared by removing as much as possible xenoliths and phenoxenocrysts by hand picking under a binocular, in order to increase the relative percentage of zeolites. The powders were ground to a grain size of 20 μm. XRD analyses were carried out by a Bruker D8 Advance X-ray diffractometer in Bragg-Brentano geometry with an anti-scatter screen, without rotation of the sample between 8 and 16° 2 θ and rotation of the sample between 16 and 66° 2θ, a LynxEye detector with an opening angle of 2.945°, primary and secondary soller slits of 2.5° and a divergence slit of 0,300 mm. Cu-Kα X-rays were generated at 40 kV and 40 mA. Phases were identified by Bruker Eva 2.0 software and the crystallographic databases ICDD PDF2 (2011) and ICSD (2011). The XRD analyses for the identification of the mineralogical composition were carried out at 20 °C/40% RH. Additionally, in order to check whether any chemical transformation occurs due to RH changes, XRD diffraction analyses were carried out at different RH's. First, the RH was increased, with steps of 10% RH, from 40 to 90%, and then lowered again, with similar steps, to 10% RH.

The physical properties of the tuff stones were studied by a combination of methods and techniques. The water absorption of the stone at 20 °C/50% RH was measured, according to EN 13755 [23], on cubes $10 \times 10 \times 10\ cm^3$, sealed with epoxy resin on the lateral sides. Additionally, the wetting front in the stones was photographically monitored on unsealed specimens. After absorption, the specimens were fully saturated by immersion in water and then dried at 20 °C/50% RH through one surface. Their weight was monitored at regular time intervals during drying.

The porosity of the stones was measured according to the RILEM CPC 11.3 on $4 \times 4 \times 4\ cm^3$ cubes [24]. Additionally, porosity and pore size distribution were measured in twofold by Mercury Intrusion Porosimeter (MIP) using a Micrometrics Autopore IV9500A. By the use of this instrument pore entrances of diameter size between 0,007 and 366 μm can be measured. Smaller pores were measured by nitrogen adsorption (Micrometrics Tristar 3000 Adsorption Analyzer); adsorption and desorption curves were measured at 77 K (−196 °C).

The thermal and hygric dilation were determined on $4 \times 4 \times 16\ cm^3$ specimens. The thermal dilation between 10 °C, 20 °C, 30 °C and 40 °C was measured by means of a dilatometer with a precision of 0.001 mm, after conditioning the specimens at each temperature in a climatic cabinet. Similarly, the hygric dilation was measured after conditioning the specimens at different RH conditions (30%, 50%, 65% and 93%) and in water, at a stable temperature of 20 °C. Additionally, hygric dilation was continuously monitored by means of linear variable differential transformers (LVDT) (measuring range 2 mm) when cycling the RH between 30% (72 h) and 93% RH (24 h) at a constant temperature of 20 °C during 12 days.

The flexural and compressive strength of the stone was assessed on $4 \times 4 \times 16\ cm^3$ specimens, according to EN 196-1 [25], before and after the weathering test. In both cases, the mechanical tests were carried out on dry specimens. The load was applied with a speed of 300 N s^{-1} and a pre-loading 10 N.

The weathering test was designed to reproduce the wet-dry cycles to which tuffstone mullions and window sills are subjected when positioned in building masonry. The test set-up developed to this purpose (Fig. 5) consisted of:

- A frame, on which the specimens were placed, positioned on an angle in order to allow flowing away of the water.
- Two pipes with hoses to sprinkle the specimens with tap water (reproducing rain)
- Four infrared lamp to lighten and warm up the specimens (reproducing the effect of the sun)
- Thermocouples to measure the surface temperature of the specimens. The thermocouples were connected to a computer, so that the intensity of the infrared lamps could be automatically adjusted to keep the temperature constant at 40 °C during the "sunny" period.

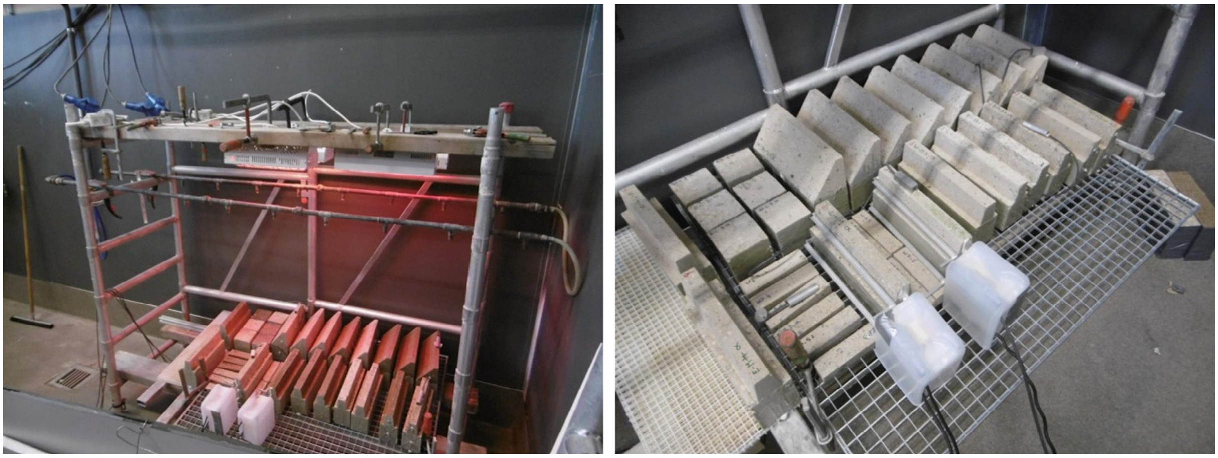

Fig. 5. Overview of weathering test (left) and specimens used for the test (right).

The following wet-dry cycle was used: 8 h rain, 64 h drying, alternating a 4 h period of drying at 40 °C (temperature at the surface of the stone) and 4 h drying at room temperature. A realistic temperature and length of rain periods were used. The length of the cycles was determined with the aim of developing a differential moisture content in the specimen during wetting and drying (in order to create the conditions for differential thermal and hygric dilation) and to repeat as much as possible cycles (in order to accelerate the occurrence of the damage). The length of the wetting and drying cycles was defined based on some preliminary tests. The specimens were sealed with resin on those sides which are normally encased in masonry. The effect of the mechanical constraint (in the building where this specific crack pattern is observed, tuff stone blocks are often partially encased in the masonry) was not reproduced in this laboratory accelerated test, because of the necessity of simplifying the set-up.

During and at the end of the weathering test, the appearance of new cracks or the widening of existing cracks was visually and photographically monitored. During the last wet-dry cycle, the moisture distribution in the exposed and encased part of mullions and window sills was assessed, after the drying and the rainy period, by drilling powder samples at different depths and determining their moisture content gravimetrically.

3. Results

3.1. Characterization tests

3.1.1. PFM

The PFM observations show that Ettringen tuff has more stone fragments (basalt, sandstone and schists) and less pumice than Weibern tuff (Fig. 6). The pumice has been zeolitized and contain inclusions of xeno- and/or phenocrysts (Ti-augite, leucite, quartz, opaque minerals, phlogopite and sanidine). Some holes are filled with calcite.

Weibern tuff shows a higher porosity than Ettringen, also due to the presence of a larger amount of pumice (Fig. 6). Next to pumice, stone fragments (sandstone, schist and silt stone) are present; these are smaller in size and lower in number than observed in Ettringen tuffstone. Xeno- and/or phenocrysts are in this case constituted by Ti-augite, quartz, biotite/phlogopite and tourmaline.

3.1.2. XRD analyses

The XRD diffraction pattern of Ettringen tuffstone (Fig. 7) shows the presence of quartz, albite, sanidine, leucite and clinopyroxene (ferroan diopside, augite, Ca-clinoferrosilite, muscovite), next to phillipsite-Ca as the only zeolite. Fitzner [26] considered phillipsite

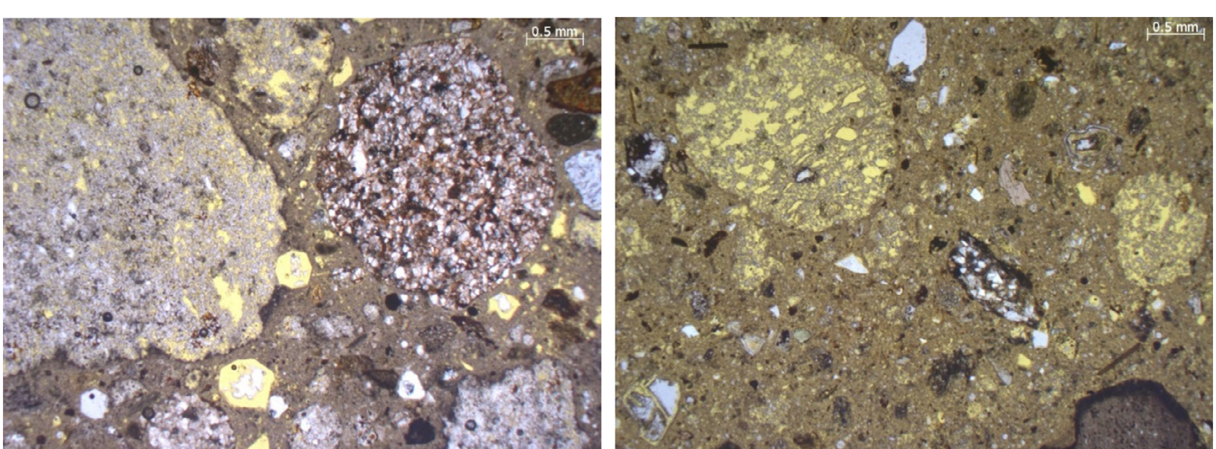

Fig. 6. Microphotographs with an overview of the microstructure of Ettringen (left) & Weibern tuff (right).

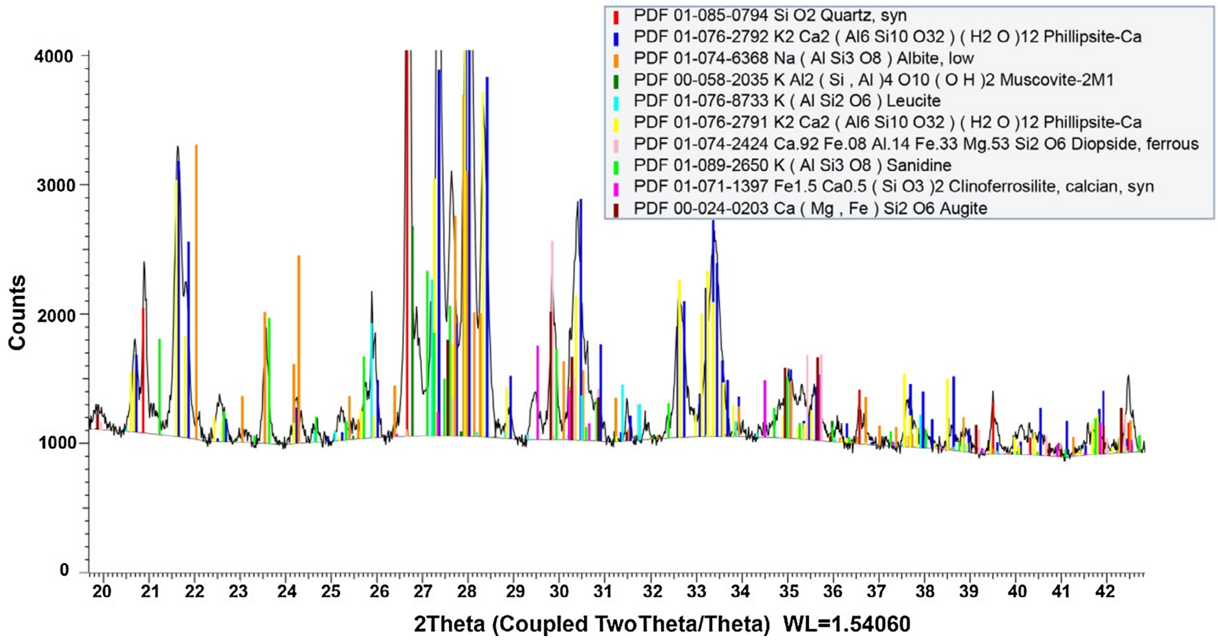

Fig. 7. The XRD pattern of Ettringen tuff, collected at 20 °C and 40 %RH.

the predominant zeolite in Ettringen tuff. The presence of phillipsite as only zeolite in Ettringen has so far only been encountered once in previous studies by our laboratory, other assemblages found are analcime, analcime + merlinoite, phillipsite + merlinoite, chabazite + phillipsite and analcime + phillipsite [8,26].

In the Weibern tuffstone, quartz, sanidine, augite, phlogopite and illite are present, next to analcime as the only zeolite (Fig. 8). This is not uncommon for Weibern tuff, in which analcime is the predominant zeolite [26]. It has been encountered as only zeolite five times in previous studies by our laboratory, other assemblages being analcime + chabazite + phillipsite and analcime + gismondine [8,26].

The XRD diffraction pattern of Weibern tuff does not change when collected at different RHs (Fig. 9). Contrarily, the XRD spectrum of Ettringen varies with RH, indicating that chemical transformations occur due to RH cycles; these differences are reversible and seem to be caused by changes in the crystal structure of phillipsite-Ca (Figs. 10 and 11).

3.1.3. Porosity and pore size distribution

The total porosity measured by saturation under vacuum according to RILEM CPC 11.3 [24] is 34.97 vol% (standard deviation 0.49) and 42.82 vol% (standard deviation 0.72) for Ettringen and Weibern, respectively.

The porosity and pore size distribution of Ettringen and Weibern tuff stones, as measured by mercury intrusion porosimeter (MIP), are reported in Fig. 12. Weibern has a higher open porosity than Ettringen, but the pore size distribution of the two stones, in

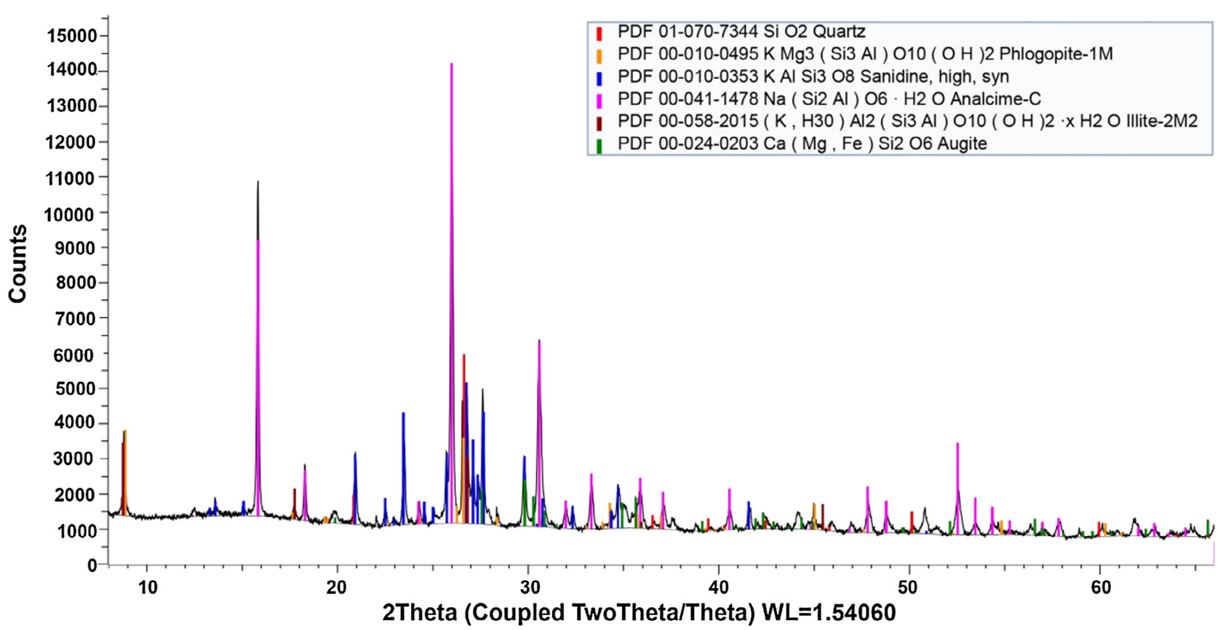

Fig. 8. The XRD pattern of Weibern tuff, collected at 20 °C and 40 %RH.

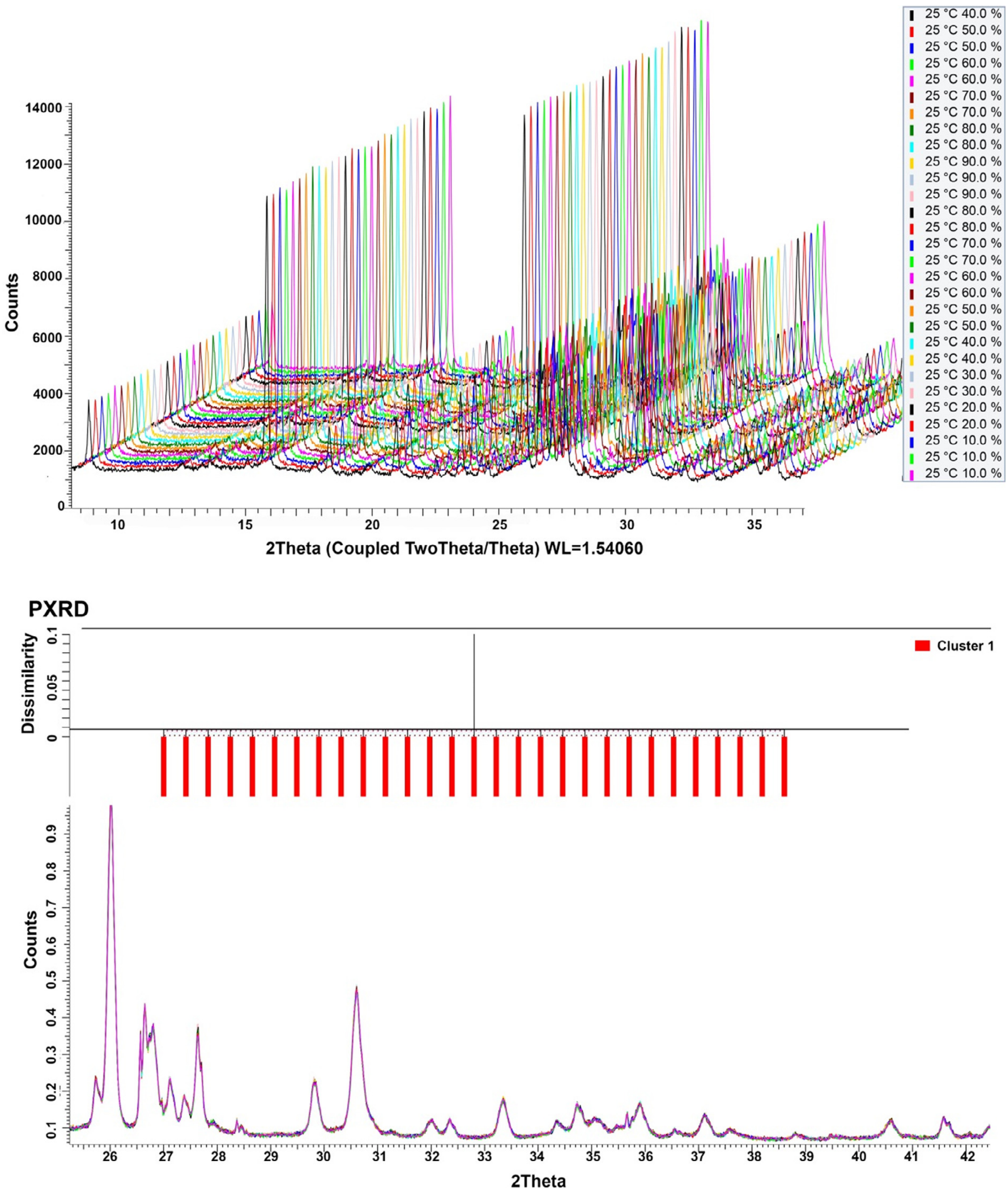

Fig. 9. XRD pattern of Weibern tuff collected at different RH's and 20 °C, in a so-called cascade plot showing all patterns (above), and in a statistical cluster analysis of the patterns (below), showing meaningful differences (in this case none) between the individual patterns over the range 10–90 % RH (compare Fig. 10).

the range measured by MIP, is similar. The open porosity values measured by MIP are in both cases (slightly) lower than those obtained by immersion, fact which might be due to the presence of pores larger than 366 μm (largest size measured by MIP) and/or to the lower representativeness of the small samples used for MIP measurements.

Pores smaller than 0.1 μm were measured by N_2 adsorption (Fig. 13). These results show that Ettringen has a larger amount of very small pores (2–4 nm) than Weibern tuff. The presence of these pores can significantly affect the hygric behaviour of this stone.

3.1.4. Water absorption and drying

Fig. 14 shows the water absorption curves of the tuff stones: Weibern has a higher total absorption than Ettringen, fact which corresponds to its higher porosity. The water absorption coefficient (WAC) of Weibern ($0.316\ kg\ m^{-2}\ s^{-0.5}$) is significantly higher than that of Ettringen ($0.064\ kg\ m^{-2}\ s^{-0.5}$), indicating the faster

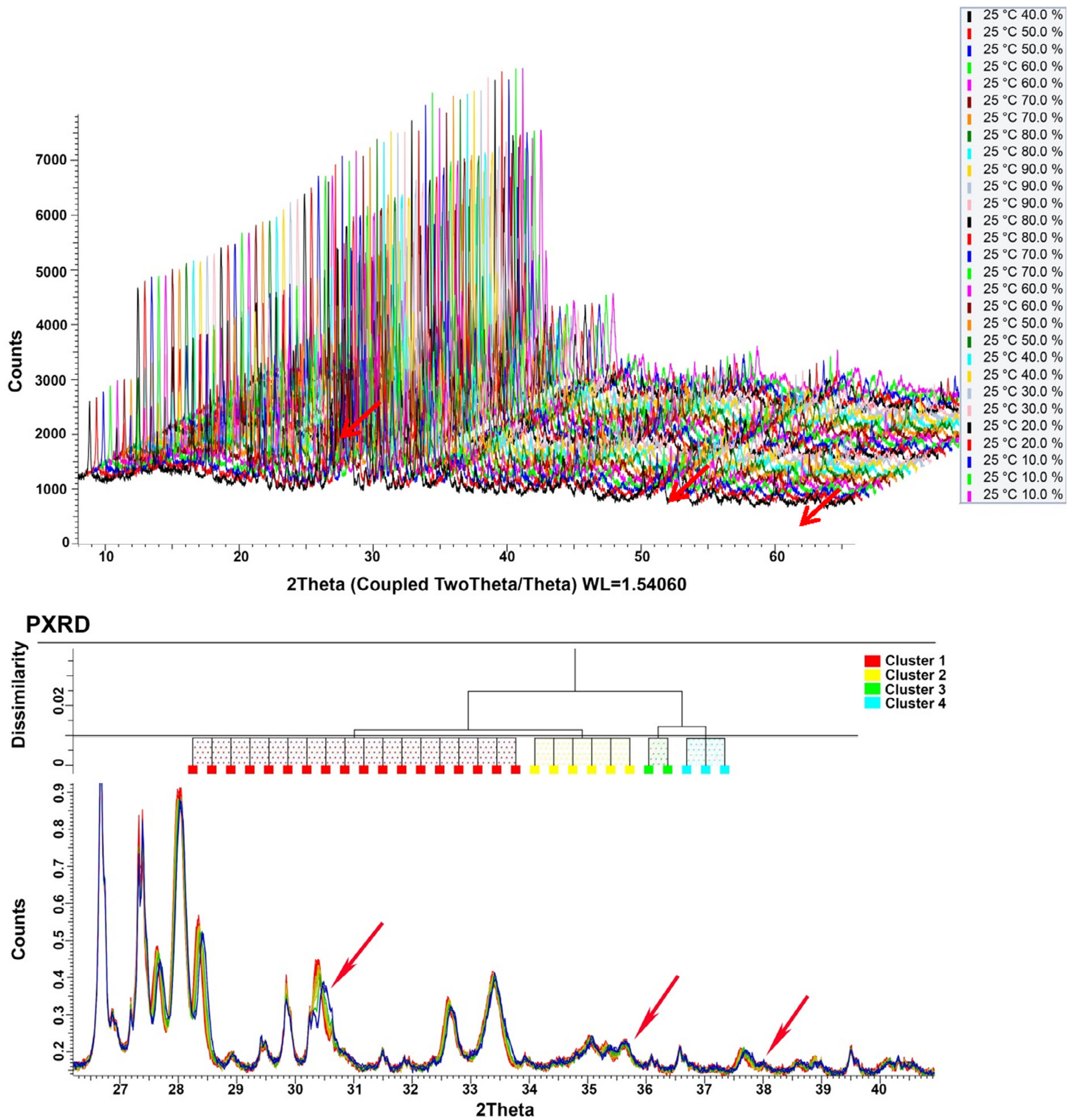

Fig. 10. XRD pattern of Ettringen tuff collected at different RH's and 20 °C, in a so-called cascade plot showing all patterns (above), and in a statistical cluster analysis of the patterns (below), showing meaningful differences between the individual patterns. Clusters 1, 2, 3 and 4 represent RH's of 60–90% RH, 30–50% RH, 20% RH and 10% RH, respectively (compare Fig. 9; also see Fig. 11).

absorption of the first with respect to the second. The measured WAC for Ettringen is slightly higher than values earlier measured in this stone type (0.05 $kg\,m^{-2}\,s^{-0.5}$, reported in [6]); the WAC measured for Weibern lies in the range reported in literature (0.24–0.38 $kg\,m^{-2}\,s^{-0.5}$, as derived based on [12,27]). During the absorption measurements it was observed that the wetting front proceeds much faster in Weibern than in Ettringen: this difference can be possibly explained by the pore structure of Ettringen (probably less interconnected than that of Weibern tuff) and/or by the presence of very small pores (2–4 nm) in Ettringen tuffstone, which delay the penetration of the wetting front. The drying of both tuff stones is slow: after more than 3 months the specimens are not fully dry yet (Fig. 15); the drying of the Ettringen stone is slower than that of Weibern.

3.1.5. Hygric and thermal dilation

The hygric dilation of Ettringen and Weibern, calculated with respect to the specimen size at 20 °C 30% RH, is given in Fig. 16. Both stones show a high hygric dilation, with a maximum of about 1.2 $\mu m\,mm^{-1}$, measured when the specimens are saturated with water by immersion. Ettringen tuffstone has a significant hygric dilation already at low RH. The hygric dilation corresponds to the hygroscopic adsorption of the specimens: Ettringen specimens, due to the presence of very small pores (see 3.1.3), start to adsorb moisture from the air already at low RH values (Fig. 17).

The reversibility of the hygric dilation was checked by continuously monitoring the dilation during few RH cycles. This test showed that the dilation is fully recovered (within the test period).

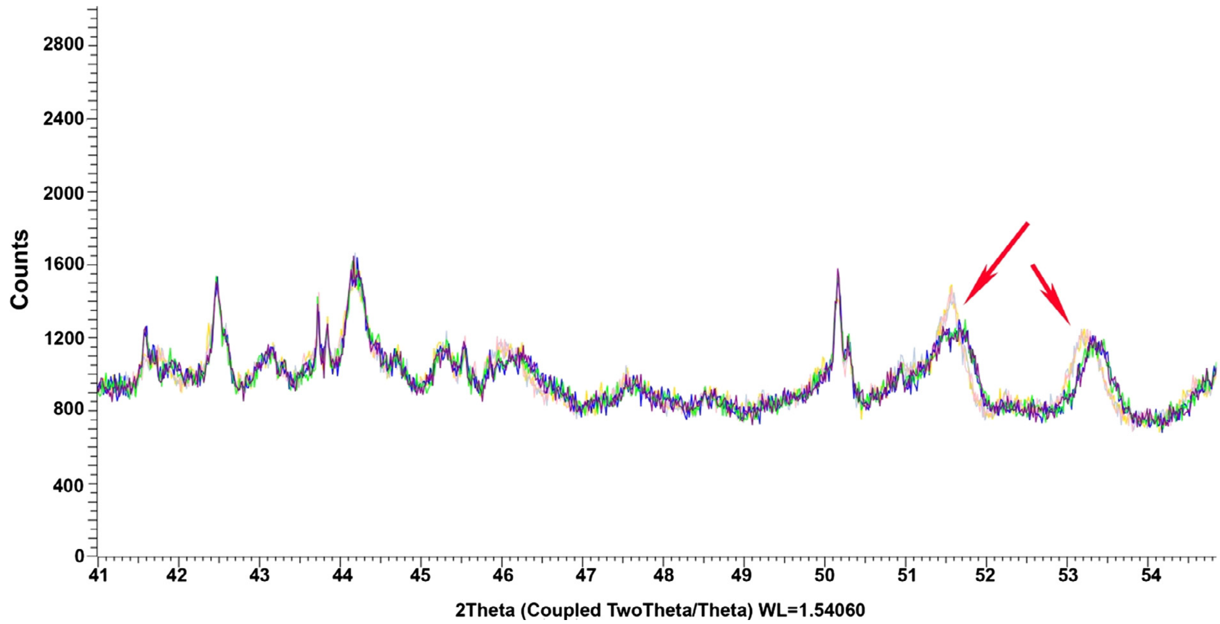

Fig. 11. Part (between 41 and 54 °2θ) of the diffraction patterns of Ettringen tuff collected at 10 and 90 %RH, respectively, illustrating the shift in the XRD pattern.

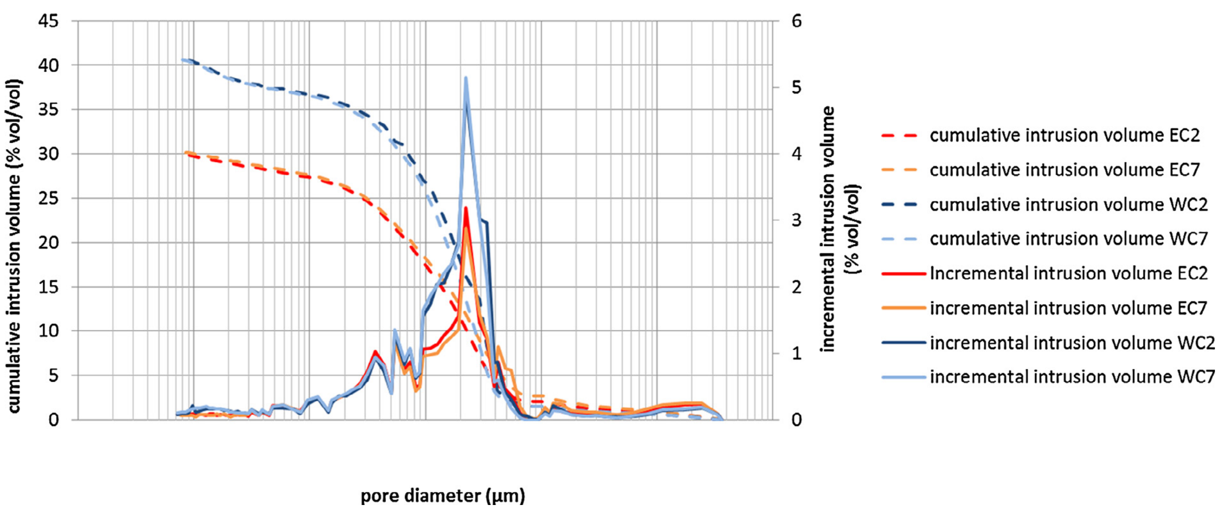

Fig. 12. Open porosity and pore size distribution of Ettringen (replicates samples EC2 and EC7) and Weibern (replicate samples WC2 and WC7) tuff stones, as measured by MIP (continuous line: incremental intrusion; dashed line: cumulative intrusion).

The thermal dilation between 10 and 40 °C at 65% RH is similar for both tuff stones and equal to 0.15 $\mu m\ mm^{-1}$; it can therefore be concluded that in these stones the thermal dilation is much less relevant for damage development than the hygric dilation.

3.1.6. Mechanical strength

The flexural and compressive strength of the stones before the weathering test is reported in Table 2. The flexural and compressive strength of Ettringen tuffstone is about double than that of Weibern. The strength values measured for Ettringen tuff show a large standard deviation, indicating that the mechanical properties of this tuffstone can significantly vary even within blocks from the same quarry.

3.2. Effect of tooling

In order to evaluate the effect of tooling, i.e. the possibility of crack initiation due to the process of chiselling of the block by the stone mason prior to weathering, samples were investigated by means of PFM observations on thin sections. Neither in the case of Ettringen tuff, nor in the case of Weibern tuff (Fig. 18), any cracks were initiated, confirming previous unpublished results on Weibern tuff.

3.3. Weathering test

The weathering test ran during about 3 months. During and at the end of this period the specimens were visually examined to check the appearance of cracks. According to the supposed damage mechanism, cracks would develop longitudinally, parallel to the exposed surface, in the exposed part of the stone elements. No cracks with these features could be observed with the naked eye. However, the randomly oriented cracks already present before the test seem, based on visual observation, to have widened up. FMA (on all specimens) and PFM (on a selection of 8 samples) observations carried out at the end of the test confirmed the

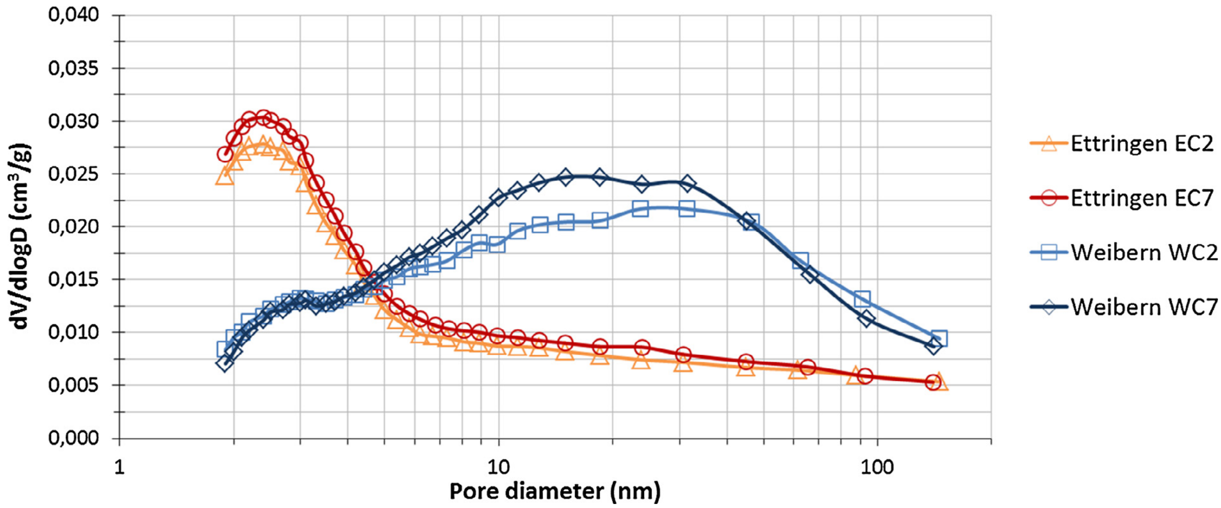

Fig. 13. Pore size distribution of Ettringen (EC2 and EC7) and Weibern (WC2 and WC7) tuff stones measured by N_2 adsorption (measurements were carried out in twofold).

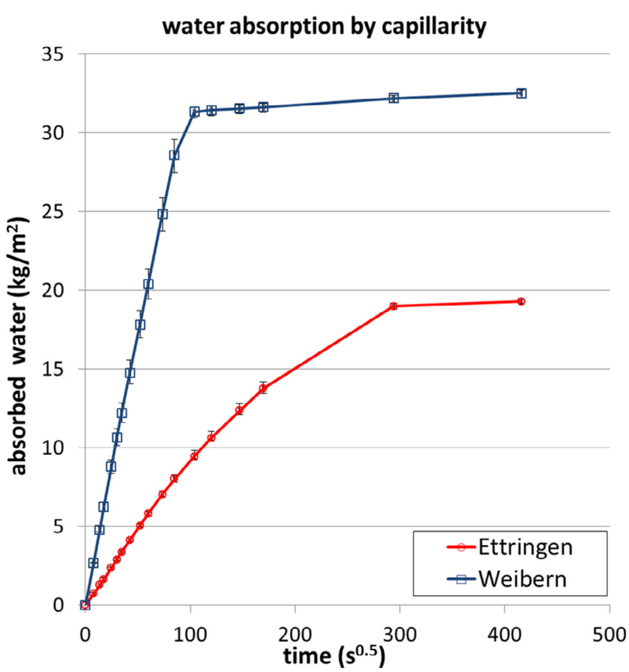

Fig. 14. Water absorption of Ettringen (E) and Weibern (W) tuff stones (average of 3 specimens).

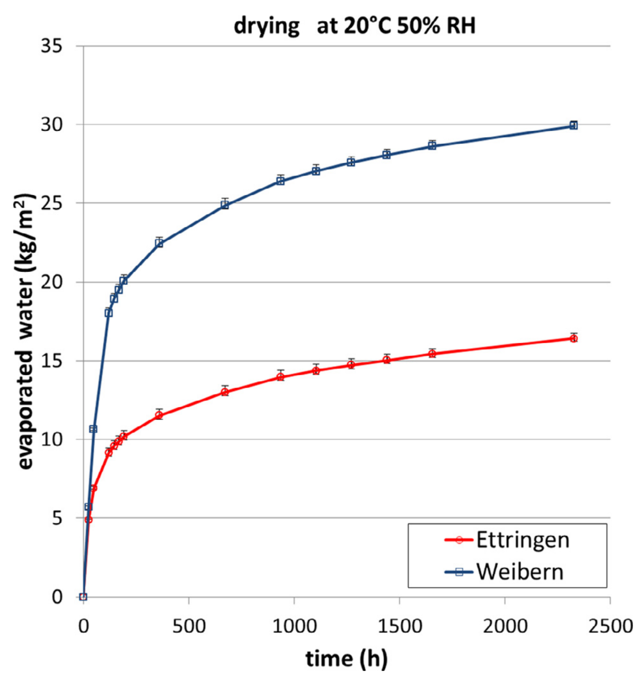

Fig. 15. Drying of Ettringen (E) and Weibern (W) tuff stones (average of 3 specimens).

absence of cracks which could be due to the supposed damage mechanism. However, it should be mentioned that the effect of the mechanical constraint was not reproduced in the laboratory weathering test, because of the necessity of simplifying the set-up. A partial encasement of the blocks, like it occurs e.g. in window sills, would have led to higher stresses at the interface between inner and outer zones with different moisture content than the situation tested in laboratory, and thus increased the risk of the development of cracks.

During the last wet-dry cycle, the moisture content in mullions and window sills, after the drying and the rain period of the cycle, was gravimetrically determined. The results (Fig. 19) show that the difference in moisture content (MC) between the encased and exposed parts can be high for both mullions and window sills. This implies that the difference in hygric dilation between exposed and encased parts can be relevant (see 3.1.5).

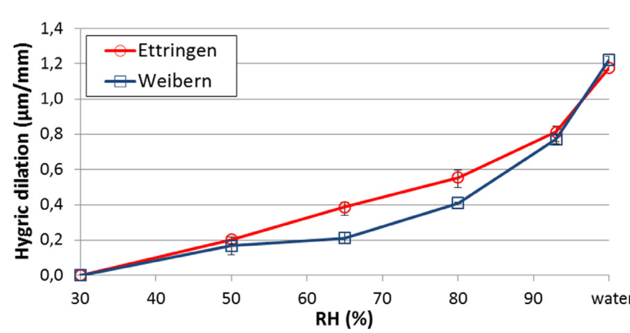

Fig. 16. Hygric dilation of Ettringen and Weibern tuff stones (average of 3 specimens).

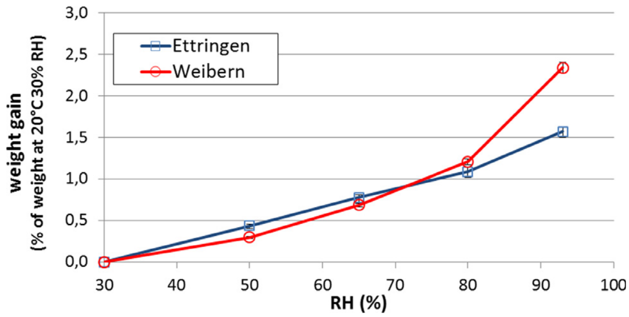

Fig. 17. Hygroscopic moisture adsorption of Ettringen and tuff stones (average of 3 specimens).

Table 2
Flexural and compressive strength of Ettringen and Weibern tuff measured before the weathering test (average of 5 specimens); the coefficient of variation [-] is reported between brackets.

	Ettringen	Weibern
Flexural strength (N/mm^2)	8.10 (0.22)	4.24 (0.10)
Compressive strength (N/mm^2)	29.41 (0.11)	13.24 (0.11)

The mechanical strength of the specimens subjected to the weathering test was assessed and compared to that measured before the test. A decrease of the flexural strength is observed for both tuffstone types at the end of the weathering test. Differently, the change of the compressive strength before and after the weathering test lies within the range of the standard deviation and is thus not significant (Table 3).

4. Discussion and conclusions

This research aimed at verifying if a differential dilation between parts of tuffstone elements with different moisture content can lead to damage in the form of longitudinal cracks between the protruding and encased part of tuffstone elements (Figs. 1 and 2). To this scope, the effect of moisture on the degradation of Ettringen and Weibern tuff has been thoroughly investigated by means of different methods and techniques. Moreover, a purpose-made weathering test has been carried out to simulate the wetting-drying process. Additionally, the hypothesis that cracks could be initiated by tooling of the stone elements, and progressively develops in time, has been evaluated by subjecting part of the samples, chiselled by a stone mason, to the same weathering test.

Despite no cracks developed during the weathering test, which could definitely confirm the supposed damage mechanism, the results obtained from the characterization tests support the hypothesis that the hygric behaviour of the stone plays an important role in the decay mechanism of Ettringen and Weibern tuff stones.

First of all, due the presence of both coarse and very fine pores, both tuff stones have a fast capillary water absorption but a very slow drying: this behaviour makes them particularly susceptible to moisture related damage mechanisms, such as biological growth, frost and salt crystallization.

Moreover, both tuff stones were shown to have a high hygric dilation; this could lead to high stresses at the interface between parts of the stone with different moisture contents, as those which develop during wet-dry cycles. These stresses are even higher in the case (part of) the stone block is constrained within the masonry structure.

In spite of the fact that the hygric dilation was shown to be reversible (at least after few RH cycles), the flexural strength of the stones slightly decreased after the weathering test, suggesting that repeated cycling would lead to weakening of the materials. Besides, the mechanical strength of these zeolite-rich tuff stones might be reduced in wet conditions [17].

Ettringen tuff seems to be more sensitive for damage than Weibern tuff, due to the presence of very fine (2–4 nm) pores, which lead to hygroscopic adsorption and hygric dilation even at low RH. As reported by Pötzl et al. [28] the presence of a microporosity in this range can play a major role in the hygric expansion of tuff stones, even in the absence of swellable clay minerals. The sensitivity of Ettringen to RH is shown also by the mineralogical changes undergone by the stone (most probably by the phillipsite-Ca in de zeolites assemblage) during RH cycles. All these factors suggest that Ettringen might be more susceptible to moisture related damage than Weibern. This high susceptibility might be (partially) compensated by its higher mechanical strength.

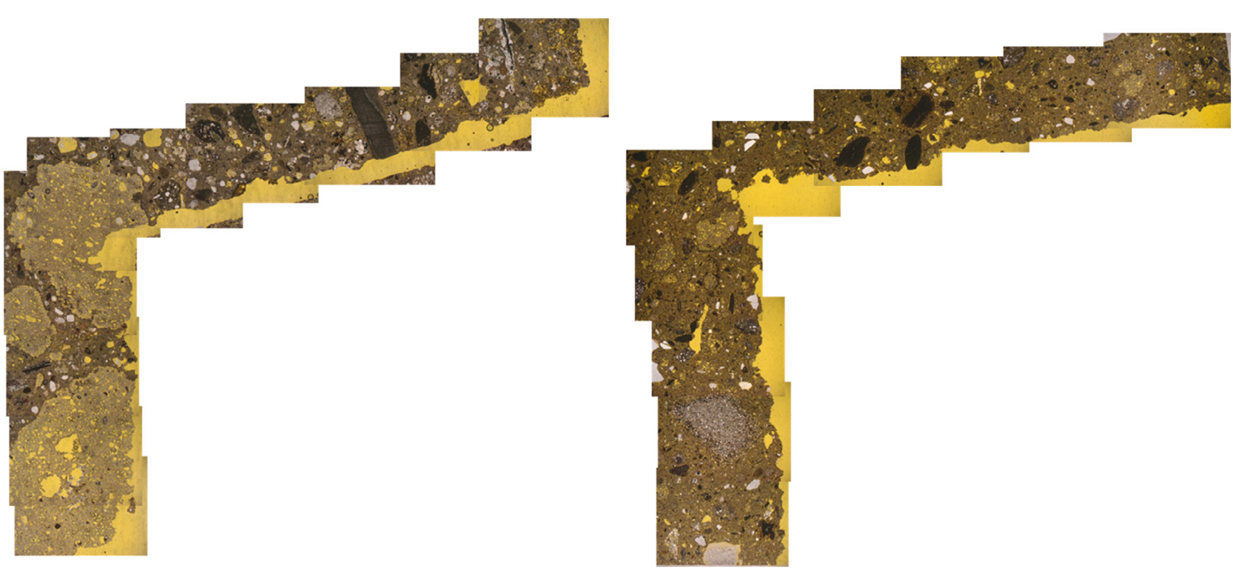

Fig. 18. Microphotographs over the bend in tooled Ettringen (left) and Weibern (right) tuff mullion. Note the absence of any microcrack.

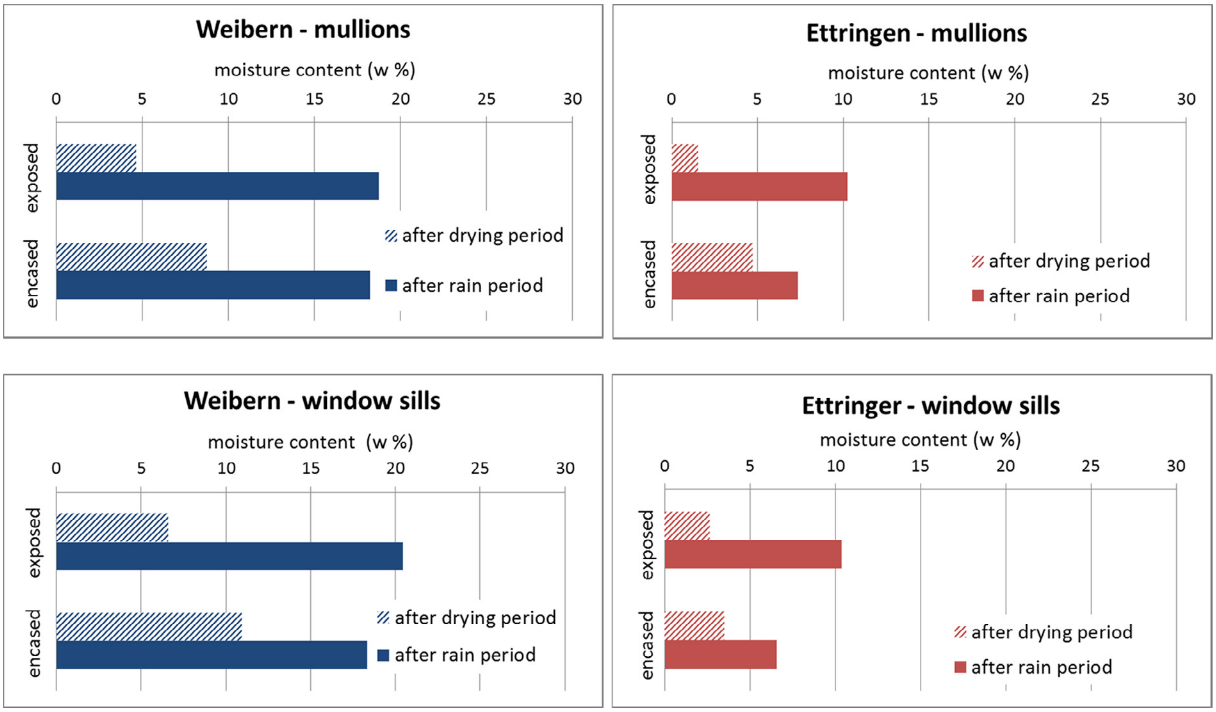

Fig. 19. Moisture content in Weibern and Ettringen mullions and window sills.

Table 3
Flexural and compressive strength of Ettringen and Weibern tuff measured after the weathering test (average of 5 specimens); the coefficient of variation [-] is reported between brackets.

	Ettringen	Weibern
Flexural strength (N/mm^2)	6.11 (0.18)	3.07 (0.18)
Compressive strength (N/mm^2)	27.65 (0.06)	14.38 (0.11)

Acknowledgements

This research is part of the programmatic collaboration MonumentenKennis (Building Conservation Knowledge), sponsored by the Dutch Ministry of Education, Culture & Science (OCW). W. Duvalois (TNO) performed XRD analyses. A. Thijssen (TU Delft) performed the MIP measurements. Patrick Verolme (Delft Solids Solutions B.V.) carried out the N2 adsorption measurements.

References

[1] C. Colella, M. de'Gennaro, R. Aiello, Use of zeolitic tuff in the building industry, in: D.L. Bish, D.W. Ming (Eds.), Natural zeolites: Occurrence, properties, applications. Reviews in Mineralogy and Geochistry 45 (2001) 551-587.
[2] G. Heiken (Ed.), Tuffs, their Properties, Uses, Hydrology, and Resources, Geological Society of America Special Paper, 2006.
[3] T.G. Nijland, W. Dubelaar, H.J. Tolboom, De historische bouwstenen van Utrecht, in: W. Dubelaar, T.G. Nijland, H.J. Tolboom (Eds.), Utrecht in Steen. Historische Bouwstenen in de Binnenstad, Matrijs, Utrecht, 2007, pp. 31–109.
[4] T.G. Nijland, R.P.J. van Hees, The volcanic foundation of Dutch architecture: use of rhenish tuff and trass in the Netherlands in the past two millenia, Heron 61 (2016) 69–98.
[5] B. Fitzner, L. Lehners, Rhenish tuff – A widespread, weathering-susceptible natural stone, in: D.G. Price (Ed.), Proceedings of the 6th International Congress of the International Association of Engineering Geology, Balkema, Rotterdam, 1990, pp. 3181–3188.
[6] W.D. Grimm, Bildatlas wichtiger denkmalgesteine der bundesrepublik deutschland. Bayerisches landesamt für denkmalpflege, München. Arbeitsheft 50 (1990).
[7] J. Helms, J.F. Johnstrup, J.F., Danske tufstens-kirker, Band. 1. De med vulkansk tuf fra Rinen byggede kirker i Tyksland, Holland og isaer i Danmark: med bemaerkninger om den rinske vulkanske Tuf. Hagerups, Copenhagen, 1894.
[8] R. Dreesen, M. Dusar, Volcanic tuff: an exotic historical building stone in Flanders, in: T.G. Nijland (Ed.), Use and Conservation of Rhenish Tuff in the Netherlands, Germany, Flanders and Denmark. Proceedings of the Symposium in Amersfoort, March 20, 2017, TNO, Delft, 2017, pp. 33–45.
[9] T.G. Nijland, S. Brendle, R.P.J. van Hees, G.J.L.M. de Haas, Decay of Rhenish tuff in Dutch monuments. Part 1: use, composition and weathering, Heron 48 (2003) 149–166.
[10] R.P.J. van Hees, S. Brendle, T.G. Nijland, G.J.L.M. de Haas, H.J. Tolboom, Decay of Rhenish tuff in Dutch monuments. Part 2: laboratory experiments as basis for the choice of restoration stone, Heron 48 (2003) 167–177.
[11] P. Schubert, B. Fitzner, O. Schwab, J. Zallmanzig, Mauerwerk aus Tuffstein, Landesinstitut für Bauwesen und angewandte Bauschadenforschung Nordrhein-Westfalen, Aachen, 1982.
[12] C. Franzen, P.W. Mirwald, Moisture content of natural stone: static and dynamic equilibrium with atmospheric humidity, Environ. Geol. 46 (2004) 391–401.
[13] W. Wedekind, R. López-Doncel, R. Dohrmann, M. Kocher, S. Siegesmund, Weathering of volcanic tuff rocks caused by moisture expansion, Environ. Earth Sci. 69 (2013) 1203–1224.
[14] R. Cioffi, O. Marino, G. Mascolo, The physical action of water on the decay of building grey-tuff stone, Mater. Eng. 2 (1991) 263–275.
[15] A. Langella, D. Calcaterra, P. Cappelletti, A. Colella, M. de' Gennaro, R. de Gennaro, Preliminary contribution on durability of some macroporous monumental stones used in historical towns of Campania region, southern Italy, in: V. Fessina (Ed.), Proceedings of the 9th International Congress on Deterioration and Conservation of Stone, Venice, 2000, pp. 59–67.
[16] M.F. La Russa, S.A. Ruffolo, M. Alvarez de Buergo, M. Ricca, C.M. Belfiore, A. Pezzino, G.M. Crisci, The behaviour of consolidated Neapolitan yellow Tuff against salt weathering, Bull. Eng. Geol. Environ. 76 (2017) 115–124.
[17] M.J. Heap, J.I. Farquharson, A.R.L. Kushnir, Y. Lavallée, P. Baud, H.A. Gilg, H.T. Reuschlé, The influence of water on the strength of Neapolitan Yellow Tuff, the most widely used building stone in Naples (Italy), Bull. Volcanol. 80 (51) (2018).
[18] J.D. Blacic, Hydration swelling effects on time-dependent deformation of zeolitized tuff, J. Geophys. Res. 98B (1993) 15909–15917.
[19] R. López-Doncel, W. Rubén, R. Wedekind, S. Dohrmann, Siegesmund, Moisture expansion associated to secondary porosity: an example of the Loseros Tuff of Guanajuato, Mexico, Environ. Earth Sci. 69 (2013) 1189–1201.
[20] B. Lubelli, T.G. Nijland, Effect of moisture on tuff stone degradation, in: K. Kielsgaard Hansen, C. Rode, L.O. Nilsson (Eds.), Proceedings of the International RILEM Conference on Materials, Systems and Structures in Civil Engineering 2016, Segment on Moisture in Materials and Structures, August 22-24 2016, Lyngby, 2016, pp. 87–96.
[21] J. Frenchen, Siebengebirge am Rhein, Laacher Vulkangebiet, Maargebiet der Westeifel. Vulkanisch-petrographische Exkursionen. Sammlung geologischer Führer 56. 2nd ed., Börntrager, Berlijn & Stuttgart, 1971.

[22] L. Viereck, Geologische und petrologische Entwicklung des pleistozänen Vulkankomplexes Rieden, Ost-Eifel. Bochumer geologische und geotechnische Arbeiten 17 (1984).
[23] EN 13755, Natural stone test methods - Determination of water absorption at atmospheric pressure, 2008.
[24] RILEM CPC 11.3, Absorption of water by immersion under vacuum, Mater. Struct. 12 (1979) 391–394.
[25] EN 196-1, Methods of testing cement. Part 1: determination of strength 2016.
[26] B. Fitzner, Volcanic tuffs: The description and quantitative recording of their weathered state, in: A.E. Charola, R.J. Koestler, G. Lombardi (Eds.), Lavas and volcanic tuffs: Proceedings of the International Meeting, Easter Island, 1990, ICCROM, Rome, 1994, pp. 33–51.
[27] T.G. Nijland, R.P.J. van Hees, Beoordeling van Weiberner en Römer tufsteen ten behoeve van de restauratie van de St. Janskathedraal te 's-Hertogenbosch. TNO, Delft, Unpublished TNO report 2003-CI-R0042, 2003.
[28] C. Pötzl, R. Dohrmann, S. Siegesmund, Environ. Earth Sci. 77 (2018) 188.